Received: 24 February 2020 | Revised: 23 April 2020 | Accepted: 2 May 2020

DOI: 10.1002/ar.24477

ARTICLE

The Anatomical Record | WILEY

Osteological description of casque ontogeny in the southern cassowary (*Casuarius casuarius*) using micro-CT imaging

Todd L. Green[1] | **Paul M. Gignac**[1,2,3]

[1]Department of Anatomy and Cell Biology, Oklahoma State University Center for Health Sciences, Tulsa, Oklahoma

[2]Division of Paleontology, American Museum of Natural History, New York, New York

[3]MicroCT Imaging Consortium for Research and Outreach, Fayetteville, Arkansas

Correspondence
Todd L. Green, Department of Anatomy and Cell Biology, Oklahoma State University Center for Health Sciences, 1111 W. 17th Street, Tulsa, Oklahoma, USA.
Email: todd.green@okstate.edu

Funding information
American Association of Anatomists (American Association for Anatomy); National Science Foundation, Grant/Award Numbers: 1450850, 1457180, 1725925, 1754659; Oklahoma State University Center for Health Sciences; The Company of Biologists, Grant/Award Number: JEBTF1903122; Western Interior Paleontological Society

Abstract

Extant cassowaries (*Casuarius*) are unique flightless birds found in the tropics of Indo-Australia. They have garnered substantial attention from anatomists with focus centered on the bony makeup and function of their conspicuous cranial casques, located dorsally above the orbits and neurocranium. The osteological patterning of the casque has been formally described previously; however, there are differing interpretations between authors. These variable descriptions suggest that an anatomical understanding of casque anatomy and its constituent elements may be enhanced by developmental studies aimed at further elucidating this bizarre structure. In the present study, we clarify casque osteology of the southern cassowary (*C. casuarius*) by detailing casque anatomy across an extensive growth series for the first time. We used micro-computed tomography (μCT) imaging to visualize embryonic development and post-hatching ontogeny through adulthood. We also sampled closely related emus (*Dromaius novaehollandiae*) and ostriches (*Struthio camelus*) to provide valuable comparative context. We found that southern cassowary casques are comprised of three paired (i.e., nasals, lacrimals, frontals) and two unpaired elements (i.e., mesethmoid, median casque element). Although lacrimals have rarely been considered as casque elements, the contribution to the casque structure was evident in μCT images. The median casque element has often been cited as a portion of the mesethmoid. However, through comparisons between immature *C. casuarius* and *D. novaehollandiae*, we document the median casque element as a distinct unit from the mesethmoid.

KEYWORDS

archosaur, craniofacial development, ornamentation, paleognathous birds, phenotypic complexity

1 | INTRODUCTION

Cassowaries (Aves: *Casuarius*) are large-bodied (average of 31.65–45.75 kg as adults; Heather & Robertson, 1997; Marchant & Higgins, 1990; Olson & Turvey, 2013), flightless birds that belong to the extant paleognathous lineage (e.g., also including tinamous, ostriches, rheas, kiwis, and emus). Although well known for their aggressive temperaments (Kofron, 1999; Rothschild, 1900) and ecological importance as seed dispersers (Bradford & Westcott, 2010; Bradford & Westcott, 2011; Mack, 1995; Stocker & Irvine, 1983; Webber & Woodrow, 2004), the hallmark novelties of these paleognath birds are their conspicuous cranial casques (Figure 1b), which are tall bony and

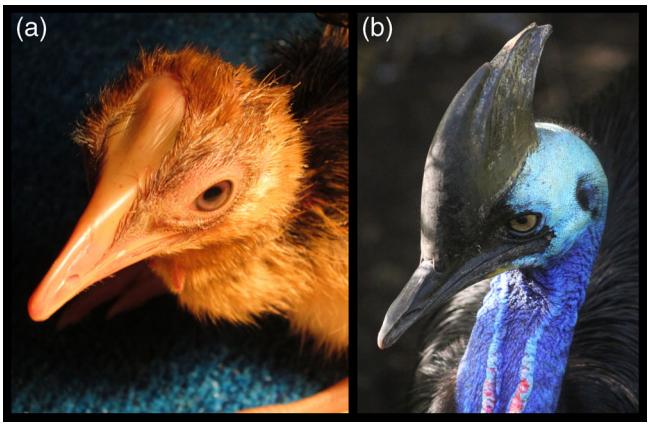

FIGURE 1 Photographs depicting the extensive soft- and hard-tissue changes that cassowaries undergo over ontogeny. (a) Southern cassowary (*Casuarius casuarius*) neonate demonstrating cranial anatomy prior to casque growth with a flattened keratinized shield on the dorsal surface of the head, extending caudally from the bill. (b) A mature *C. casuarius* with an enlarged casque, which is a keratinized and bony dorsal expansion of the shield in (a). Photos by T. L. G

keratinous protrusions that extend dorsally above the orbits and neurocranium. In cassowaries, keratinous outer sheathing generally follows the shape of the bony casque surface, though it may exceed the height of the underlying pneumatized bone (Naish & Perron, 2016; Pycraft, 1900; Richardson, 1991).

Starting in the late 19th century (Flower, 1871; Marshall, 1872; Parker, 1866; Pycraft, 1900; Rothschild, 1900), these cranial ornaments have been the subject of numerous hypotheses regarding their composition and function (Crome & Moore, 1988; Dodson, 1975; Eastick, Tattersall, Watson, Lesku, & Robert, 2019; Mack & Jones, 2003; Mayr, 2018; Naish & Perron, 2016; Phillips & Sanborn, 1994; Richardson, 1991; Starck, 1995). Interestingly, previous studies detailing the constitution of cassowary cranial casques have led to several different interpretations of their contributing bony elements. Such differences likely result from the extensive fusion and remodeling that casques undergo throughout ontogeny, thus, obfuscating clear demarcations between individual skull bones. Clarification of casque composition can, therefore, be gleaned from the use of internal imaging techniques, such as high-resolution micro-computed tomography (μCT), as well as examination of early developmental stages prior to bone fusion. Gaining this understanding would enhance our ability to infer how casque form implicates function and to test hypotheses about the biological role(s) of this unusual structure.

Formal descriptions of cassowary skulls were initially made by Parker (1866), Flower (1871), and Marshall (1872). These works identified the mesethmoid (used interchangeably with "ethmoid" by early authors) as a primary component of the casque. In fact, Parker (1866) described this constituent as the element making up the entirety of the casque. In addition to the mesethmoid, Marshall (1872) included the nasal bones as casque contributors, and Flower (1871) further described potential contributions from the lacrimals, frontals, and parietals. Although variable, each of these descriptions was based on the visual interpretation of a continuous, central bony strut passing superiorly from between the orbits. Building on these works, Pycraft (1900) performed more complete osteological investigations that comparatively sampled cassowary and non-cassowary paleognath cranial osteology. In addition to the mesethmoid, Pycraft (1900) included the nasals and frontals as casque elements based on their characteristic "inflation" (developmental expansion through invasion by adjacent pneumatic passages and extensive growth of thin trabecular bone, internally) as well as direct interfaces with the mesethmoid. Pycraft (1900) also questioned whether the unpaired element at the center of the casque was composed of the mesethmoid only: based on apparent separation between dorsal and ventral components of the bone in early developmental ages (exact ages not specified; see Plate XLIV from Pycraft, 1900), an additional, more dorsal bony element in the midline was identified. This was referred to as a "median element of the casque" (herein: median casque element), and it was specifically differentiated from the mesethmoid, which was interpreted as having a more inferior position (e.g., contributing to the interorbital septum). The homology of the median casque element was not addressed by Pycraft at the time (1900), nor has it been formally evaluated since. Together, these historical texts summarize which elements were thought to contribute to which anatomical aspect of the casque: the mesethmoid forming a rostrodorsal portion, a tentatively labeled median casque element occupying the most dorsal aspect, nasals contributing to the rostrolateral walls, lacrimals marginally involved in the base laterally, and frontals along with parietals supporting the caudolateral base. Expanding on these efforts, more recent osteological descriptions have produced other interpretations of element combinations to casque formation in cassowaries (Mayr, 2018; Naish & Perron, 2016; Richardson, 1991), resulting in the characterization of several casque phenotypes (refer Table 1 for historical interpretations).

Cassowary research has been impeded by persistent taxonomic and sampling issues. Namely, multiple species are often grouped by authors into a single *Casuarius* genus complex, which may obscure potential taxonomic differences in casque anatomy as well as our ability to identify homologs for cranial elements between cassowaries and other avians. Additionally, adult cassowary

TABLE 1 Terminology by previous authors to describe bony elements contributing to cassowary casques

Publication	Described bony elements	Species
Parker (1866)	"Ethmoid" (= mesethmoid)	*C. bennetti*
Flower (1871)	Nasals, mesethmoid, lacrimals, frontals, parietals	*C. australis* (= *C. casuarius*)
Marshall (1872)	Nasals, "ethmoid" (= mesethmoid)	*C. galetus* (= *C. casuarius*)
Pycraft (1900)	Nasals, "median element of the casque" (= median casque element), mesethmoid, frontals	*C. unappendiculatus*, *C. sclaterii* (= *C. casuarius*)
Richardson (1991)	"Calcified core" sitting atop cranial bones	*C. casuarius*
Naish and Perron (2016)	Frontals	*C.* sp. (= *C. casuarius*)
Mayr (2018)	Nasals, mesethmoid	*C. casuarius*, *C.* sp.
Green and Gignac (this study)	Nasals, median casque element, mesethmoid, lacrimals, frontals	*C. casuarius*

casque shapes and dimensions appear to be taxon-specific, introducing the possibility of variation in the bony elements contributing to the casque. Generally, southern cassowaries (*C. casuarius*) possess tall and laterally compressed casques (Figure 1b), whereas northern cassowaries (*C. unappendiculatus*) have tall trigonal casques with relatively broad caudal regions and often flattened dorsal surfaces, and dwarf cassowary (*C. bennetti*) casques are less tall trigonal pyramids (Marshall, 1872; Perron, 2016; Rothschild, 1900). Treating the genus *Casuarius* as a monolith subsumes interspecific variation into one taxonomic grouping, and may mask our understanding of how the casque grows, how cranial bones are incorporated in the casque, and how intraspecific (e.g., sexual dimorphism) or interspecific differences (e.g., from reproductive isolation) may relate to casque evolution.

In this study, we expand on prior cassowary cranial anatomical descriptions by sampling cassowary casques across ontogeny using μCT imaging. Although a dorsal keratinous shield is present in neonates where the casque will eventually grow (Figure 1a), cassowaries begin life without a casque. Therefore, we scanned a comprehensive embryonic and post-hatching growth series of southern cassowaries to track the incipient development of bony casque elements from beneath the initial keratinous shield, through casque initiation and dorsal expansion, and into skeletal maturity and adulthood. High-resolution digital imaging allowed us to identify internal suture boundaries and track patterns of inflation, which were critical for reinterpreting casque constituency. Our three aims were to (a) describe the bony cranial anatomy in *C. casuarius*, specifically, (b) clarify the identity of midline casque constituent(s) through osteological comparison with other extant ratites, and (c) describe the ontogeny of bony casque features by documenting casque inflation and growth. Using these methods, and the largest comparative and ontogenetic dataset of cassowaries to date ($n = 54$), we found that *C. casuarius* cranial anatomy is unique among major ratite groups and casque composition is more complex than previously described. This comparative and ontogenetically informed re-description of *C. casuarius* casques provides important osteological context that will enable future studies of casque evolution and function to be more directly characterized.

2 | MATERIALS AND METHODS

2.1 | Specimen sampling, acquisition, and access

We sampled 54 southern cassowaries: 12 embryonic, 22 immature, and 20 adult individuals (see below for ontogenetic stage criteria). None harbored obvious cranial abnormalities, with the exception of one embryo that possessed a single malformed eye, which was used to assist in embryonic age approximation but was not used to interpret cranial osteology. Twenty-three individuals ($n_{\text{embryonic}} = 6$, $n_{\text{immature}} = 12$, $n_{\text{adult}} = 5$) were μCT scanned to track bony cranial elements beneath the keratin sheath and within the skull. The remaining 31 (skulls without keratin along with preserved and dissected heads) were used for visual inspection of casque sutural boundaries or aging assessments ($n_{\text{embryonic}} = 6$, $n_{\text{immature}} = 10$, $n_{\text{adult}} = 15$). Data from adult and immature *C. casuarius* specimens were collected from the American Museum of Natural History (AMNH; New York, NY), Cassowary Conservation Project (CCP; Fort Pierce, FL), Denver Museum of Nature and Science (DMNS; Denver, CO), Melbourne Museum (Museums Victoria, MV; Melbourne, VIC, Australia), Museum of Osteology (MOO; Oklahoma City, OK), Natural History Museum (NHMUK; Tring, UK), Queensland Museum (QM; Brisbane, QLD, Australia), Sedgwick County Zoo (SCZ; Wichita, KS), and T. L. Green Research Collection (TLG; Tulsa, OK). Individuals from the breeding and

zoological institutions were collected fresh, whereas museum specimens were fluid-preserved or skeletonized. Institutional care protocol was not required as all specimens were collected as cadaveric after death. No individuals were harmed or sacrificed for the purpose of this study.

To describe changes in osteology over development, we also surveyed the literature (e.g., Maxwell, 2009; Pycraft, 1900; Zusi, 1993) and sampled non-casqued paleognaths: 19 emus, *Dromaius novaehollandiae* ($n_{\text{embryonic}} = 5$, $n_{\text{immature}} = 6$, $n_{\text{adult}} = 8$) and 13 ostriches, *Struthio camelus* ($n_{\text{embryonic}} = 1$, $n_{\text{immature}} = 10$, $n_{\text{adult}} = 2$). *Dromaius novaehollandiae* specimens were donated by Dream Acres Emu Ranch (DAER; Cheyenne, WY), Rabbit Creek Emu Ranch (RCER; Livermore, CO), S. Sarno (WEL; Wellington, CO), Sugar Maple Emus (SME; Monroe, WI), Valley View Emus (VVE; Fennimore, WI), and Y. Brockdorf (HLB, Hillsboro, OR). *Struthio camelus* specimens were donated from Colorado Gators (CG; Mosca, CO), Krehbiels Specialty Meats (KSM; McPherson, KS), Longneck Ranch (LNR; Rose Hill, KS), and Pueblo Zoo (PBZ; Pueblo, CO). As with the *Casuarius* specimens, no birds were killed or harmed for the purpose of this study, and all specimens were collected opportunistically after death. Samples were frozen on site and shipped frozen to Oklahoma State University Center for Health Sciences (OSU-CHS; Tulsa, OK); where they were stored in freezers (−20°C). Nine specimens were dissected in laboratories at OSU-CHS and Colorado State University (CSU; Fort Collins, CO) and cleaned through the use of dermestid beetles or warm water maceration at CSU to view bony cranial surfaces. A full list of adult and immature specimens can be found in Data S1.

Embryonic specimens were attained from breeding institutions and university collections. Unhatched cassowary eggs ($n = 8$) were donated by the CCP. Emu eggs ($n = 5$) were collected from DAER, RCER, and VVE. One ostrich embryo was obtained from LNR. Eggs with embryos that did not develop fully and died in-shell during the incubation process were stored (at −10° C) and then shipped frozen. Eggs were thawed, eggshells were cut carefully away, embryos were removed from yolk and vitelline membrane, and extraneous fluids were removed from carcass surfaces. Extracted embryos were then refrozen or chemically fixed, and four *C. casuarius* and three *D. novaehollandiae* individuals were μCT imaged. Additional embryonic cassowary specimens were provided by the WitmerLab at Ohio University (Ohio University Vertebrate Collection, OUVC; Athens, OH) as μCT datasets ($n = 2$), by the Gladys Porter Zoo (GPZ; Brownsville, TX) as a fixed specimen ($n = 1$), and by the CCP as a disarticulated skeleton ($n = 1$). A full list of embryonic specimens can be found in Data S1.

2.2 | Identification of southern cassowary specimens

All adult specimens were confirmed as *C. casuarius* according to the criteria of Marshall (1872), Rothschild (1900), and Perron (2016), including preserved and/or soft-tissue records that are synapomorphic for the species *C. casuarius* (e.g., two wattles, species-specific coloration patterns). *Casuarius casuarius* maintain distinct casques that appear more similar to conspecifics than to other species (i.e., *C. unappendiculatus*, *C. bennetti*; Marshall, 1872; Rothschild, 1900; Perron, 2016), therefore; skeletal-only adult specimens with little data ($n = 7$) were categorized as *C. casuarius* based specifically on this narrow casque shape. For younger, immature individuals with no or incipient casques, known breeding or detailed collection histories were a prerequisite for inclusion in this study.

2.3 | Specimen preparation

Wet specimens were μCT scanned either as frozen, fixed in 10% neutral buffered formalin, or fixed in 70–95% ethanol. Preparation information can be found in Data S1. All specimens were packaged in lightweight foam and polyethylene plastic for scanning. Prior to egg processing, embryos were identified within intact eggs via two-dimensional (2D) X-ray imaging. This allowed for targeted dissection of eggs containing embryos across different stages of development.

2.4 | μCT data collection

Image data were collected on four μCT scanning systems: (a) a 2010 GE phoenix v|tome|x s240 high-resolution microfocus computed tomography system (General Electric, Fairfield, CT) housed in the Microscopy and Imaging Facility of the AMNH; (b) a 2012 Nikon XT H 225 ST μCT system (Nikon Metrology, Brighton, MI) housed at the Dentsply Research and Development Office (Dentsply; Tulsa, OK); (c) a 2018 Nikon XT H 225 ST μCT system housed at the MicroCT Imaging Consortium for Research and Outreach (MICRO; Fayetteville, AR); and (d) a TriFoil Imaging eXplore CT 120 Small Animal X-Ray CT Scanner (TriFoil Imaging, Chatsworth, CA) at the Ohio University MicroCT Scanning Facility (OUμCT; Athens, OH).

Scanning parameters varied based on system optimizations; see Data S1 for parameter listings.

2.5 | Digital reconstruction of μCT data

Tagged Image File Format (TIFF) stacks of CT-generated data were cropped of extraneous background pixels to minimize file volumes, and stitched along the Z-axis if necessary (e.g., for "tall" scans), using the program ImageJ (v. 1, US National Institutes of Health, Bethesda, MD). Digital models of bony cranial elements were three-dimensionally (3D) reconstructed in the program Avizo (versions 9–version 9.7; Visualization Science Group, Burlington, MA; Thermo-Fisher Scientific; Waltham, MA) and Avizo Lite (version 2019; Thermo-Fisher Scientific) by automatic and manual segmentation of bone-specific greyscale values. Two-dimensional slices and 3D digital bony models were examined for external and internal anatomy to determine cranial configuration, suture boundaries, bony fusions, and extent of bony inflation.

2.6 | Age and osteological definitions utilized in this study

It is necessary to outline criteria for aging southern cassowary individuals to appropriately organize an ontogenetic series from samples spanning multiple sources with differential age indicators available. Similarly, we propose explicit criteria for those traits that constitute participation of cranial bones into the casque as well as how to identify if, or when, such contributions shift across ontogeny.

Because some specimens were unaccompanied by known ages, we develop aging criteria that also enable us to approximate stepwise acquisition of casque element contributions through ontogeny. Our criteria for embryonic, immature, and mature classifications are qualitative, such as extent of ossification and integumentary traits. Other criteria include measurements of non-casque skull features to estimate relative ages within each of our three age categories. Osteological specimens were measured with a 300-mm Stainless Steel Absolute Digital Caliper (Taylor Toolworks, Columbia, MO). Linear measurements were taken for skull length (from the rostral tip of the premaxilla to the caudalmost extent of the supraoccipital bone) in mm (see Figure 2 for cranial osteological terms). These measurements were also made for digital samples (in mm) with the "Measurements" functions in Avizo and Avizo Lite. Criteria for embryo, immature, and mature aging follow, along with inclusion/exclusion criteria for elements contributing to the casque.

2.6.1 | Embryo aging criteria

Embryonic cassowaries are defined herein as individuals that died within an egg, excluding those that died during hatching after the eggshell was perforated. Southern cassowaries have an egg incubation process that ranges from 48 to 56 days (Romagnano, Hood, Snedeker, & Martin, 2012) and emus range from 46 to 56 days (Minnaar & Minnaar, 1992; 50 days on average, Minnaar & Minnaar, 1998). Exact time of death for embryos was unknown due to opportunistic collection. The embryology of *C. casuarius* has not been described previously although embryology of a sister group, *D. novaehollandiae*, has been (e.g., Maxwell, 2009; Minnaar & Minnaar, 1998; Nagai et al., 2011). Therefore, emus were used as suitable analogs for approximating embryonic developmental stage identification in cassowaries. We assessed relative stages (Hamburger Hamilton Stages, HH; Hamburger & Hamilton, 1951) and ages by documenting embryonic *C. casuarius* anatomies and comparing them to a suite of characters from previous *D. novaehollandiae* studies with known termination ages. These included, (a) external physical characteristics (Nagai et al., 2011), (b) tibiotarsus/embryo length (Minnaar & Minnaar, 1998), and (c) cranial ossification patterns (Maxwell, 2009; Data S1). Although the later HH stages (i.e., 40–44) are largely based on bill and digit lengths from embryonic domestic chickens (*Gallus gallus*; Hamburger & Hamilton, 1951), our approximations within this range were made via comparative external morphological characteristics and metrics of emus (Minnaar & Minnaar, 1998; Nagai et al., 2011).

2.6.2 | Immature aging criteria

Immature individuals include those newly hatched (neonate; inclusive of egg-bound individuals that perforated the eggshell) through sub-adulthood individuals (described below). None were sexually mature at the time of death. For the purposes of this study, we define sexual maturity as the age at which viable offspring can be produced. Osteological indicators for immature individuals include qualitative features common to neognaths and paleognaths (Kesteven, 1942; Maxwell, 2008, 2009; Pycraft, 1900): incomplete ossification of the interorbital septum with incomplete contributions from the mesethmoid (fused or unfused at this stage), frontals, laterosphenoids, and basiparasphenoid complex (at this

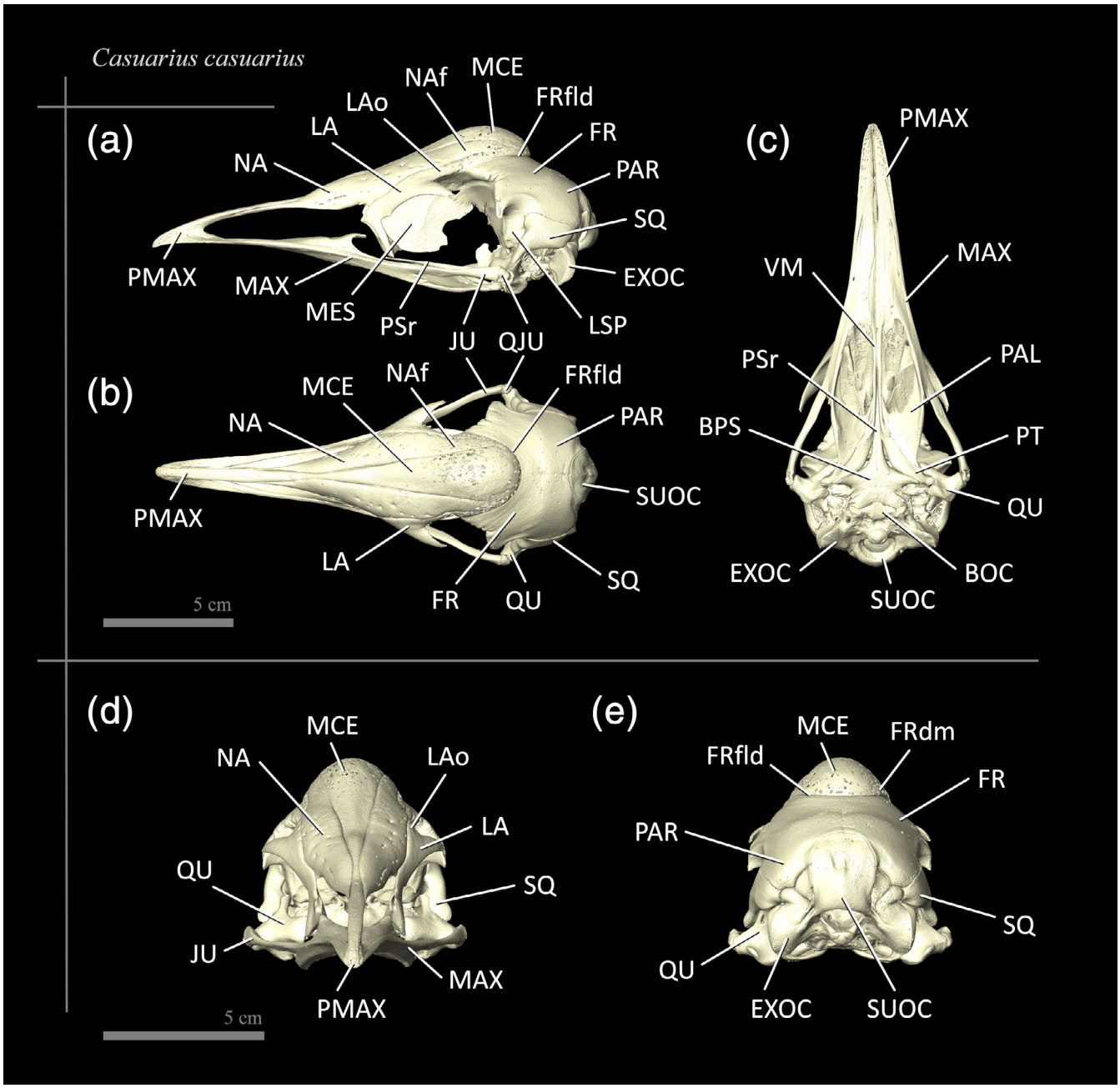

FIGURE 2 Digital rendering of the cranial osteology of an immature 10.4-month-old *Casuarius casuarius* (TLG C004) in (a) left lateral, (b) dorsal, (c) ventral, (d) rostral, and (e) caudal views. BOC, basioccipital; BPS, basiparasphenoid; EXOC, exoccipital; FR, frontal; FRdm, dorsalmost margin of the frontal; FRfld, frontal fold; JU, jugal; LA, lacrimal; LAo, orbital process of lacrimal; LSP, laterosphenoid; MAX, maxilla; MCE, median casque element; MES, mesethmoid; NA, nasal; NAf, frontal process of nasal; PAL, palatine; PAR, parietal; PMAX, premaxilla; PSr, parasphenoid rostrum; PT, pterygoid; QJU, quadratojugal; QU, quadrate; SQ, squamosal; SUOC, supraoccipital; VM, vomer. See Data S1 for additional specimen information

stage parasphenoid and basisphenoid may be unfused or fused with one another). Soft-tissue secondary sexual characteristics for immature individuals include brown feathers and incomplete apteria coloration (e.g., non-contiguous regions of blue, red, and purple; Rothschild, 1900). Subadults, for example, will have begun to transition to adult coloration, but they lack the fully black feathers and well-developed apteria with brightly colored skin of the head and neck, which characterizes adults. If exact age was not known, immature specimens were arranged into an ontogenetic sequence by increasing skull length.

2.6.3 | Mature aging criteria

This category exclusively includes individuals that were reproductively capable or listed as adults in museum databases. Cranial osteological indicators of maturity are common to neognaths and paleognaths (Parker, 1866; Pycraft, 1900; Zusi, 1993), notably, complete ossification of the interorbital septum with contributions from the mesethmoid (fully fused), frontals, laterosphenoids, and basiparasphenoid. Soft-tissue secondary sexual characteristics for mature individuals include completely black feathers and full apteria coloration (e.g., contiguous regions of blue, red, and purple; Rothschild, 1900). The reproductive status of mature individuals was also confirmed by donating sources when possible (Data S1). Mature specimens were arranged first by age (for those known), and then by increasing head length into an ontogenetic sequence. Notably, the most mature male cassowaries do not attain the same body sizes as the most mature females (see Olson & Turvey, 2013), resulting in the largest individuals in the sample represented exclusively by female specimens. Further large-sample studies should be developed to test *C. casuarius* growth trajectories.

2.6.4 | Definition of osteological traits for bones contributing to casque

Previous studies indicate that bones may contribute fully or partially to osteological ornaments (see Mayr, 2018), therefore, we defined casque participation as bones that exhibit direct physical association with the structural composition of the ornament. Specifically, a bony element can participate partially (e.g., as a single process supporting the base of the casque) or fully (i.e., with the entire element involved in the ornament structure). In cassowaries, the ornament is generally considered as a series of osteological expansions dorsal of the orbit and neurocranium. We utilized non-casqued *D. novaehollandiae* and *S. camelus* as a basis of comparison to identify dorsal expansion beyond that of other paleognathous birds. Birds have highly pneumatized bones generally, and this holds true for casques as well (Brassey & O'Mahoney, 2018; Starck, 1995). However, it is important to note that many other bones within the avian skull can also be pneumatized (Witmer, 1990). Therefore, although the degree of inflation may be used as supporting evidence for casque contribution (e.g., compared to less pneumatized adjacent bones), it was not used as a standalone observation for the purpose of defining casque contribution in this study.

2.6.5 | Definition of osteological traits for bones not contributing to casque

Bones that do not exhibit direct physical association with the structural composition of the casque are excluded from our definition of casque composition. Specifically, these are cranial bones which neither fully nor partially provide structure or support to the casque (i.e., no single process or region of the element provides structure to the casque nor its base). Excluded bones are therefore expected to share their relative sizes and shapes with homologous bones in closely related, non-casqued taxa.

3 | RESULTS

3.1 | Casque elements in southern cassowaries

Due to incomplete bony element fusion, immature specimens proved to be particularly informative for determining casque composition. These individuals capture important stages after casque elements have become well ossified but prior to the point when multi-element fusion begins. Sutures are patent and visible in immature individuals, facilitating identification of individual bony elements and their boundaries (Figure 2).

We found a total of eight elements that participate in casque composition during ontogeny: three paired (left and right nasals, lacrimals, and frontals) and two unpaired bones (median casque element and mesethmoid; Figure 3). As exemplified by the immature individual in Figure 3, the rostral and rostrodorsal portions of the casque consist of the nasals laterally and median casque element medially and superiorly. Each extends caudally, dorsal of the orbits. The caudal two-thirds of the nasals (including the frontal processes of the nasals; Baumel & Witmer, 1993) extend to the caudal border of the orbit, contributing to the rostrolateral casque walls. The entirety of the median casque element continues beyond the caudal orbital margin and forms the most caudal extent of the casque. The orbital processes of the lacrimals (Baumel & Witmer, 1993; Maxwell, 2008) contribute to the lateral bases of the casque, whereas the dorsalmost margins of the frontals form the lateral and caudolateral bases. Both appear to support the more dorsally located elements (Figures 3 and 4a). The frontals contact the lacrimal bones, nasal bones, and median casque element along their dorsalmost margins (Figures 2e and 3a,d), and they provide the inferior platform for the caudal casque. This occurs as the dorsally

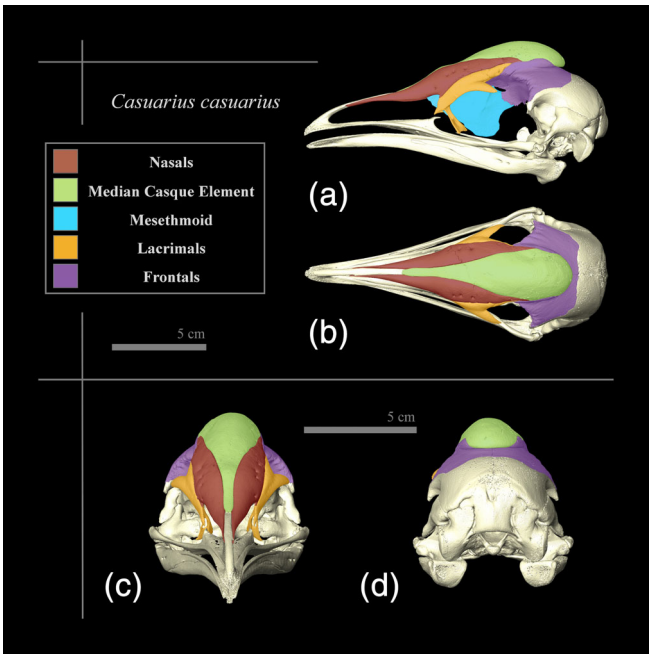

FIGURE 3 Digital rendering representing the cranial osteology of a 14-month-old immature *Casuarius casuarius* (TLG C031) in (a) left lateral, (b) dorsal, (c) rostral, and (d) caudal views with casque bones false colored (maroon = nasals; green = median casque element; blue = mesethmoid; orange = lacrimals; purple = frontals; see Data S1 for additional specimen information)

projecting and inflated frontal bones grow to "fold" over-top themselves (referred to hereafter as an osteo-developmental fold), forming an acute angle between the projection and the skull table contribution of the frontals (Figure 2a,b,e). The mesethmoid occupies an internal-only placement and cannot be seen in dorsal view. However, it becomes inflated like its neighbors, and the dorsalmost portion of the mesethmoid provides support as the central, internal base of the casque (Figure 4a). Notably, in *C. casuarius*, the mesethmoid is more dorsally expanded compared to *D. novaehollandiae* and *S. camelus* of similar ages, consistent with our interpretation of its inclusion into the casque structure (Figure 4). The nasals and median casque element comprise the greatest contributions to the casque in mature individuals, whereas those of the lacrimals, frontals, and mesethmoid are less elaborate (Figure 3).

3.2 | Bony cranial anatomy in embryonic specimens

In the embryonic cassowary samples (e.g., Figures 5a, i–ii and 6; ~HH40, TLG C032; ~HH41, TLG C030; see Data S1) no cranial ornament was present. None of the eight elements that will eventually make up the casque are fused in embryos, and none are dorsally inflated (Figures 5a, i–ii and 6). Moreover, the mediocaudal portions of the frontals are not fully formed, leaving a relatively large, caudodorsal fontanel in the neurocranium that is present medially between the frontals and parietals (Figure 6).

The mesethmoid is a T-shaped bone that forms the rostralmost portion of the ossified interorbital septum and contributes to the nasal septum in some avian species (Baumel & Witmer, 1993). The early ontogeny of the mesethmoid has been described previously in emus (Maxwell, 2009) but not in cassowaries. Consistent with emus described in Maxwell (2009), we find that southern cassowaries possess two embryonic ossification centers for the developing mesethmoid (the interorbital septum inferiorly and lamina dorsalis superiorly; Figure 5), which form a similar T-shaped, midline element when fused. The interorbital septum of the mesethmoid forms first, as seen in TLG C032 (~HH40) and the laminae dorsalis forms second as exemplified in TLG C030 (~HH41). At approximately stage HH41, these mesethmoid ossification centers remain distinct in *C. casuarius* (Figure 5a,ii; TLG C030), while the mesethmoid is fully fused in our comparably staged *D. novaehollandiae* sample (Figure 5b, i; TLG E139). Drawing from our ossification and morphometric data, along with Maxwell (2009), suggests that the appearance of the two separate mesethmoid ossification centers may occur earlier than HH41 in *D. novaehollandiae*. Nonetheless, it has been indicated that the timing of mesethmoid ossification may be highly variable between individuals (Maxwell, 2009), which points toward a need to formally examine this pattern further using additional specimens of known ages. Additionally, the ossifying mesethmoid of *D. novaehollandiae* is perforate, whereas that of *C. casuarius* is not in any of the embryonic stages analyzed in this study (Figure 5). In *D. novaehollandiae*, this fenestra developmentally closes later in ontogeny (Kesteven, 1942; Parker, 1866; Pycraft, 1900) to more greatly resemble the mesethmoid of *C. casuarius*.

In addition to the mesethmoid, southern cassowaries uniquely possess a second, dorsalmost, and horizontal midline bone, the median casque element (Pycraft, 1900). This bone is distinct from the lamina dorsalis of the mesethmoid, such that all three ossifications (i.e., both laminae of the mesethmoid and the median casque element) can be identified simultaneously in our cassowary embryos (Figures 5ii and 6e). No comparable third bony structure is known for either *D. novaehollandiae* or *S. camelus*, and we are not aware that it has ever been identified in embryos of other paleognathous birds.

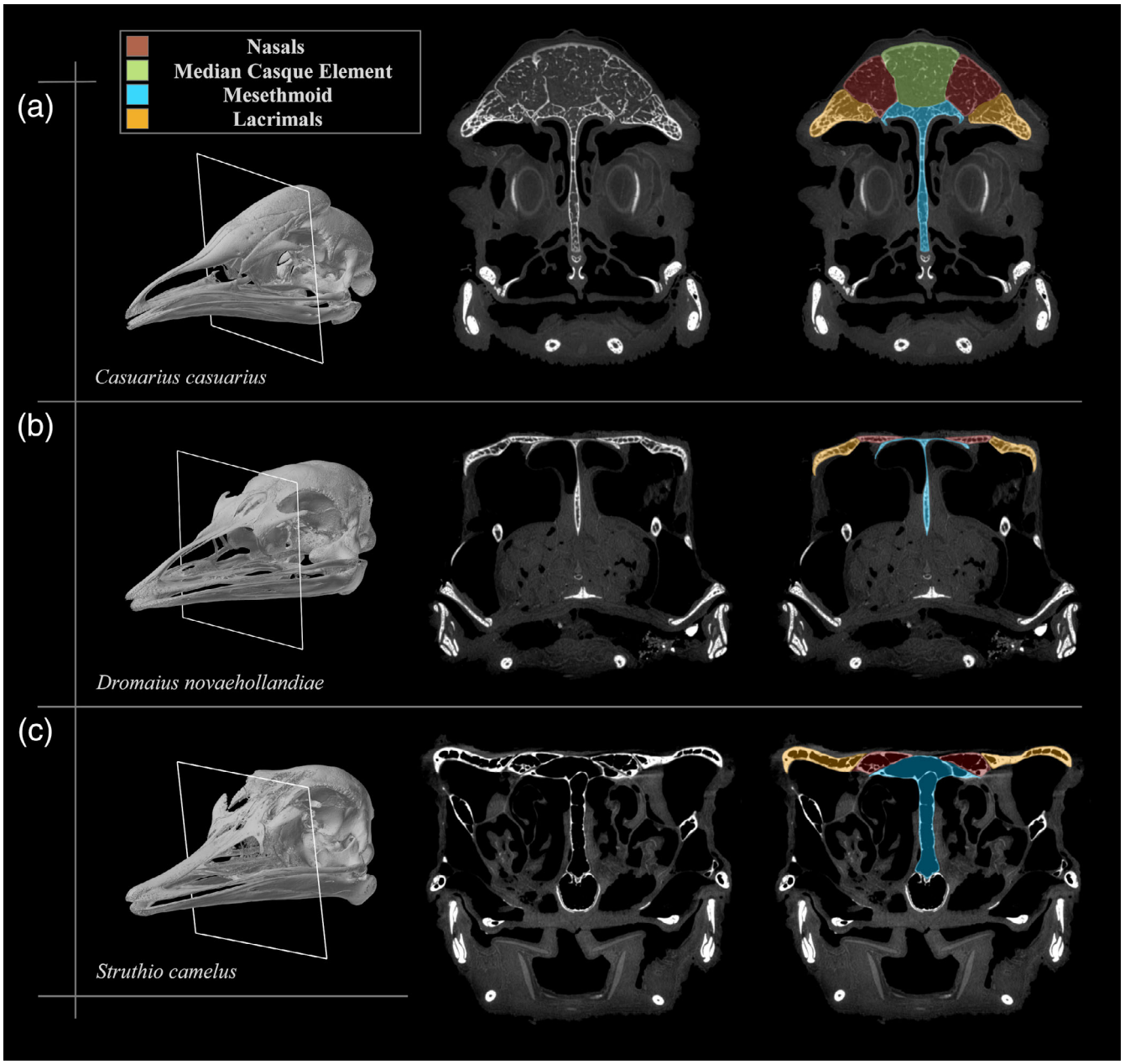

FIGURE 4 μCT transverse sections through skulls (left column; white squares) of an immature (a) *Casuarius casuarius* (TLG C031; 14.0 months old), (b) *Dromaius novaehollandiae* (TLG E115; 12.0 months old), and (c) *Struthio camelus* (TLG SC063; 15.0 months old). CT sections (middle column) are false-colored (right column) to illustrate the inclusion of the mesethmoid (blue) and lacrimals (orange) as casque components in *C. casuarius* based on increased dorsal expansion compared to non-casqued ratites. (For additional specimen details see Data S1; maroon = nasals; green = median casque element)

3.3 | Bony cranial anatomy in immature specimens

Of the three broad age classes, immature individuals characterize the morphological changes important for identifying casque elements and understanding the progression of casque ontogeny. During immaturity, individuals progress from a casque-less skull to one with a rudimentary, incipient casque and ultimately reach a phenotype that includes a moderately raised dome, consisting of several paired and midline elements. For the purposes of clarifying our results, therefore, we subdivided immature individuals into three phases of growth based on osteological traits: Phase 1, prior to elemental inflations and fusions; Phase 2, after incipient elemental inflation but prior to elemental fusions; and Phase 3, after the onset of both elemental inflation and fusion.

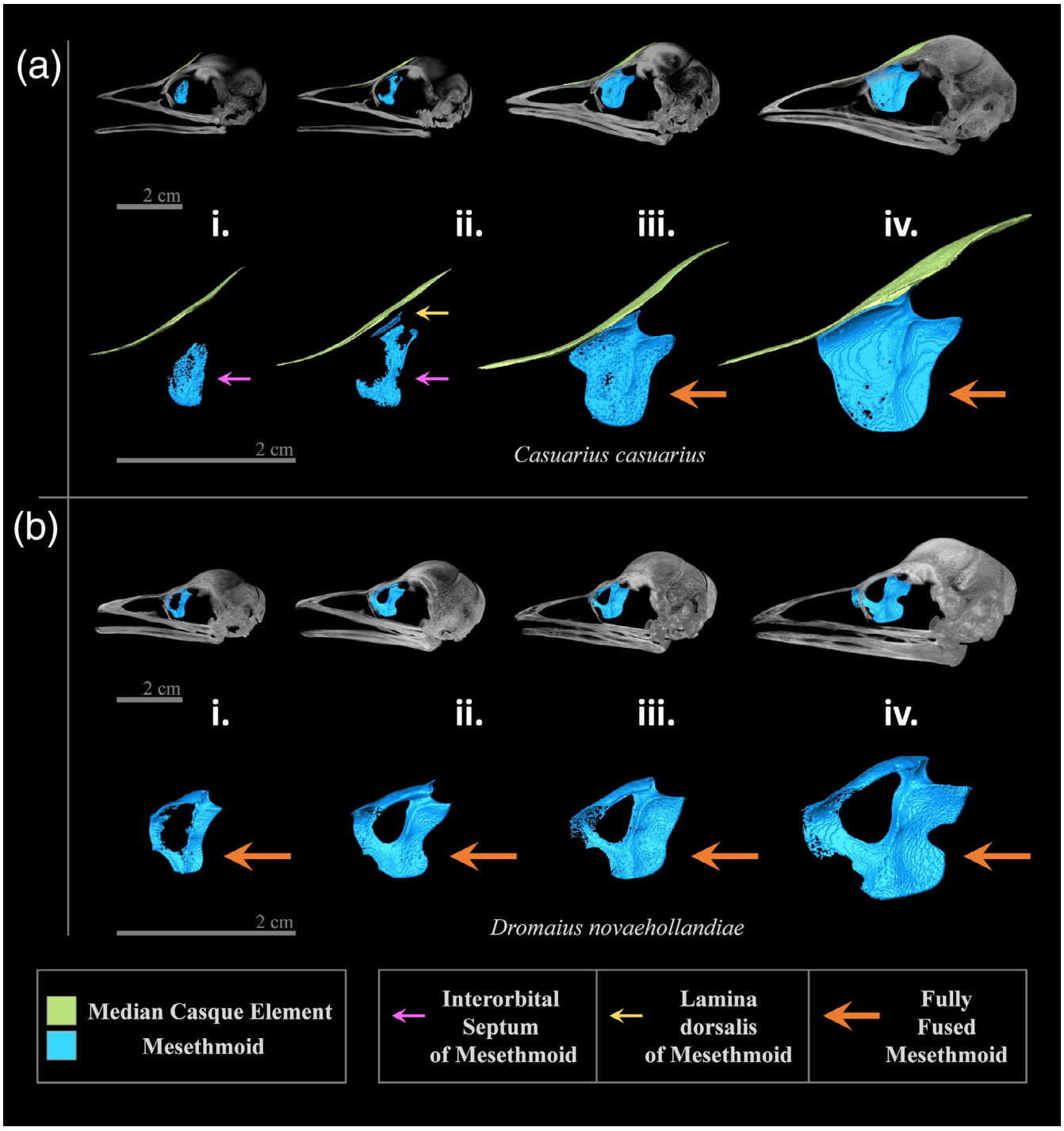

FIGURE 5 Left lateral view of digital renderings of select skull elements (green = median casque element; blue = mesethmoid ossifications) from early development in (a) *Casuarius casuarius* (i = embryonic, ~HH40, TLG C032; ii = embryonic, ~HH41, TLG C030; iii = immature, 7 days old, TLG C025; iv = immature, 1.5 months old, TLG C037) and (b) *Dromaius novaehollandiae* (i = embryonic, ~HH41, TLG E139; ii = embryonic, ~HH45, TLG E137; iii = immature, 5 days old, TLG E093; iv = immature, 1.0 month old, TLG E098) with intraspecific samples arranged by skull sizes. Comparisons to *D. novaehollandiae* illustrate that the *C. casuarius* median casque element is a distinct bone from the mesethmoid. Colored arrows indicate specific components of the developing mesethmoid: small purple arrows = interorbital septum ossification center of the mesethmoid; small yellow arrow = lamina dorsalis ossification center of the mesethmoid; large orange arrows = ossification centers joined as a contiguous mesethmoid bone (see Data S1 for additional specimen information)

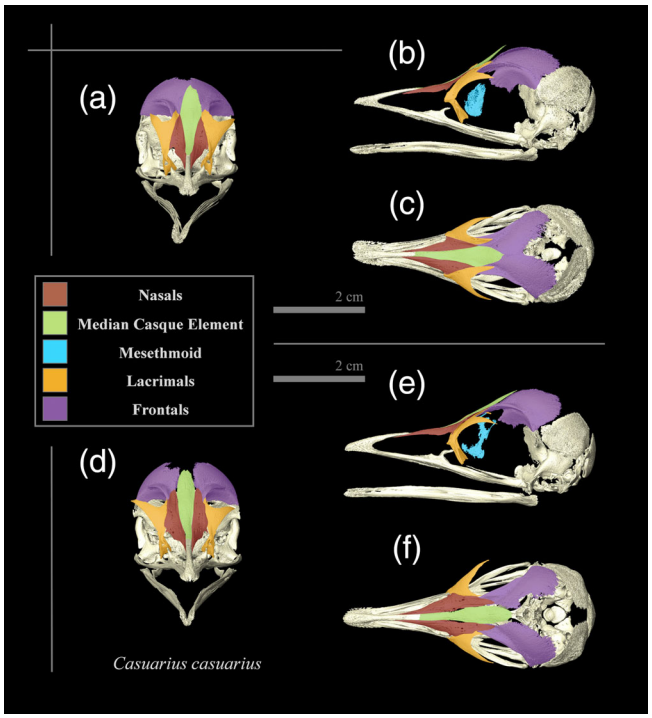

FIGURE 6 Digital rendering of embryonic *Casuarius casuarius* at stages (a–c) ~HH40 (TLG C032) and (d–f) ~HH41 (TLG C030). Skulls are rendered in (a, d) rostral, (b, e) left lateral, and (c, f) dorsal views with elements that will contribute to casque as false colored (maroon = nasals; green = median casque element; blue = mesethmoid and/or mesethmoid ossification centers; orange = lacrimals; purple = frontals; due to the soft nature of TLG C032, the frontals artificially overlapped at the dorsal midline during μCT imaging; see Data S1 for additional specimen information)

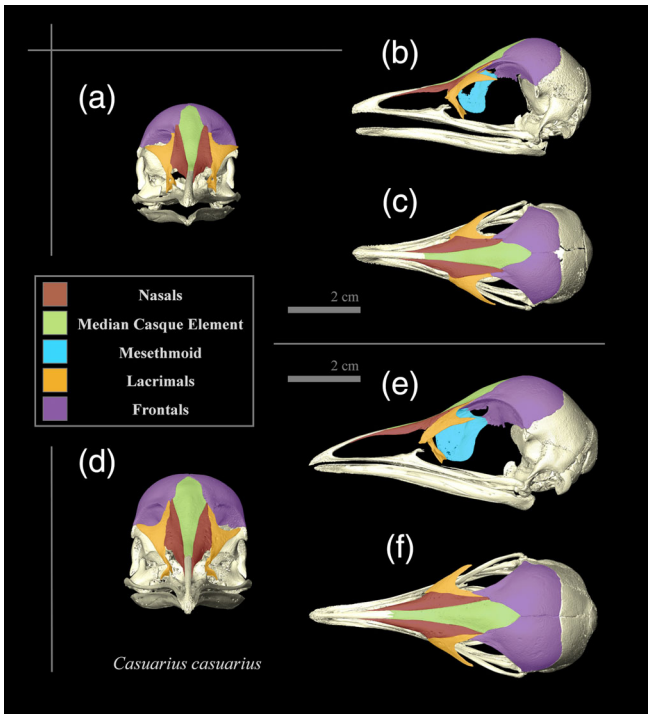

FIGURE 7 Digital rendering of immature *Casuarius casuarius* skulls at (a–c) 1 day (TLG C010) and (d–f) 1.5 months of age (= 47 days; TLG C037). Skulls are rendered in (a, d) rostral, (b, e) left lateral, and (c, f) dorsal views with elements that will contribute to the adult casque colored (maroon = nasals; green = median casque element; blue = mesethmoid; orange = lacrimals; purple = frontals; see Data S1 for additional specimen information)

3.3.1 | Immature: Phase 1

Immature individuals at this phase demonstrate cranial elements that will contribute to the casque in older individuals but are not yet fused or inflated, thus, failing to meet the criteria set for casque formation. Neonate *C. casuarius* skulls (see Figure 5a, iii; TLG C025, 7 days old; Figure 7a–c, TLG C010, 1 day old; also see Data S1) are reminiscent of the neonate *D. novaehollandiae* phenotype (see Figure 5b, iii; TLG E093; 5 days old; also see Data S1), particularly in lateral view. However, there are exceptions when viewed dorsally, including a more laterally compressed rostrum, frontal processes of the nasals that extend further caudally to the midpoint of the orbit, and the presence of an enlarged, dorsal, and rostrocaudally oriented median casque element visible at the midline surface of the skull (Figures 5 and 6). As ossification of the mesethmoid becomes complete, it also lengthens in a rostrocaudal direction, deep to the median casque element. The dorsalmost region of the mesethmoid also becomes more pneumatized as compared to an emu of similar age (i.e., 7–24 days old), gaining loosely spaced trabecular bone (Figure 8a, i). Despite this, there is not yet an indication of inflation for any bones dorsal to the orbital margins (Figures 5a and 8a, iii). Because this fails to meet our definition for casque formation at this age, it appears that pneumatization of cranial bones occurs prior to their inflation as an incipient casque. Additionally, ossification of the frontals continues mediocaudally during this period as the caudodorsal fontanel begins to close Figure 7c.

3.3.2 | Immature: Phase 2

Immature individuals at this phase have elements, which have begun inflating (Figures 5a, iv, 7d–f, 8b, 9 and 10c, d), but do not show obliteration of sutures between bones comprising the casque. In our ontogenetic series, 1.5 months is the youngest individual (TLG C037; Data S1) for which we detected inflation of any casque element (Figure 8b). The nasals, median casque element, and

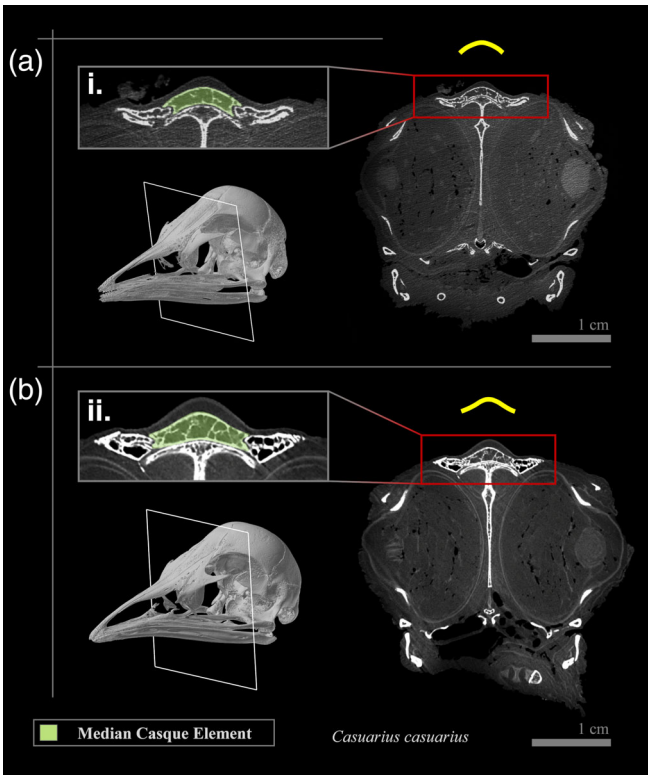

FIGURE 8 Two- and three-dimensional μCT skull projections of *Casuarius casuarius* specimens (a) (TLG C043; 42 days old) and (b) (TLG C037; 1.5 months old). 3D skulls (left) indicate locations of transverse sections (white squares) that correspond to 2D slices (right, with reticle indicating enhanced view). Small red rectangles contain areas of interest for the initial inflation of the casque, and larger grey rectangles are enlarged views of (i) a condition that although pneumatized is unelaborated and (ii) a condition that is both pneumatized and elaborated (indicating an incipient casque). Highlighted osteology (green) represents median casque elements. Yellow lines illustrate the overall shape of the dorsal surface of the median casque element before (top) and during (bottom) initial casque initiation, changing from a simple to a flared convexity in transverse view (See Data S1 for additional specimen information)

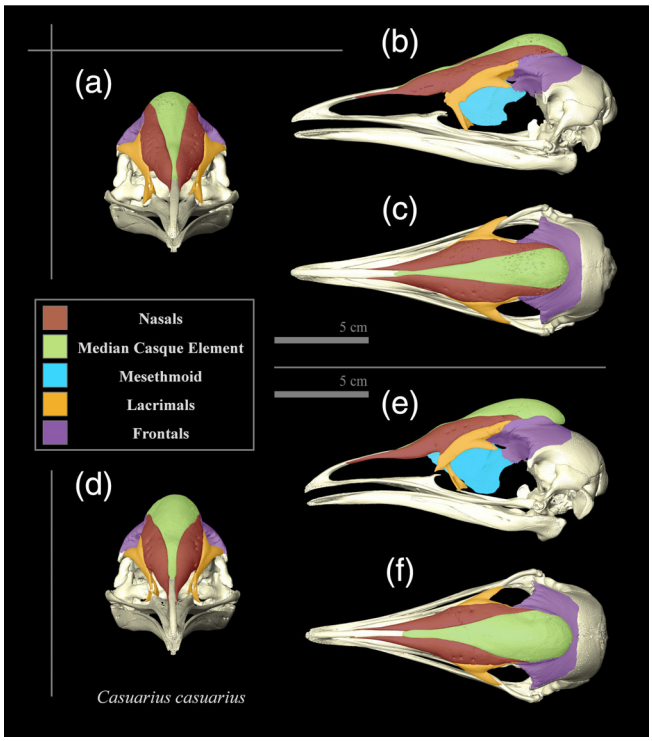

FIGURE 9 Digital rendering of immature *Casuarius casuarius* at (a–c) 10.4 months (TLG C004) and (d–f) 14.0 months of age (TLG C031). Skulls shown in (a, d) rostral, (b, e) left lateral, and (c, f) dorsal views with elements that contribute to casque false colored (maroon = nasals; green = median casque element; blue = mesethmoid; orange = lacrimals; purple = frontals; see Data S1 for additional specimen information)

mesethmoid inflate first (Figures 5a,iv, 8b, and 10c). The origin of this inflation appears to derive medially at the median casque element and mesethmoid, which subsequently pneumatized the nasals laterally (Figure 8b, ii). This progression is evident inside these four individual bones as loosely spaced trabeculae proliferate while these elements expand dorsal to the orbit. Externally, the median casque element changes shape from concave to weakly sinusoidal in lateral view (Figure 5a). In transverse section, the dorsal surface of the median casque element changes from a simple convexity (Figure 8a) to take on a laterally flared, and dorsally expansive profile (Figure 8b). In this phase the frontals ossify at their caudomedial margins to fully border the parietals, and no caudodorsal fontanel is present.

The earliest individual for which we observed all casque elements to be at least partially inflated was 10.4 months of age (Figures 2 and 9a–c; TLG C004). In this individual the nasals, median casque element, mesethmoid, lacrimals, and frontals now show at least some degree of inflation and, as a result, contribution to the casque structure. However, contribution of the orbital processes of the lacrimals is minimal (Figures 2 and 9a–c). As a unit the casque has begun to expand laterally and caudally (Figure 9a–c). In particular, the lateral pneumatized expansions of the nasals contact and begin to inflate the orbital processes of the lacrimals. The frontal processes of the nasals and median casque elements both elongate caudally and contribute to the inflation of the frontals (Figures 2 and 9a–c). In this individual the dorsalmost margins of the frontals that contribute to the caudolateral casque have started to grow in a manner that reflects a flat surface folding onto itself (Figure 11a–c, iv–vi) over the caudodorsal surface of the frontals (Figures 3 and 9a–c). The loosely spaced trabeculae within the casque now take on a distinctly "honeycombed" appearance.

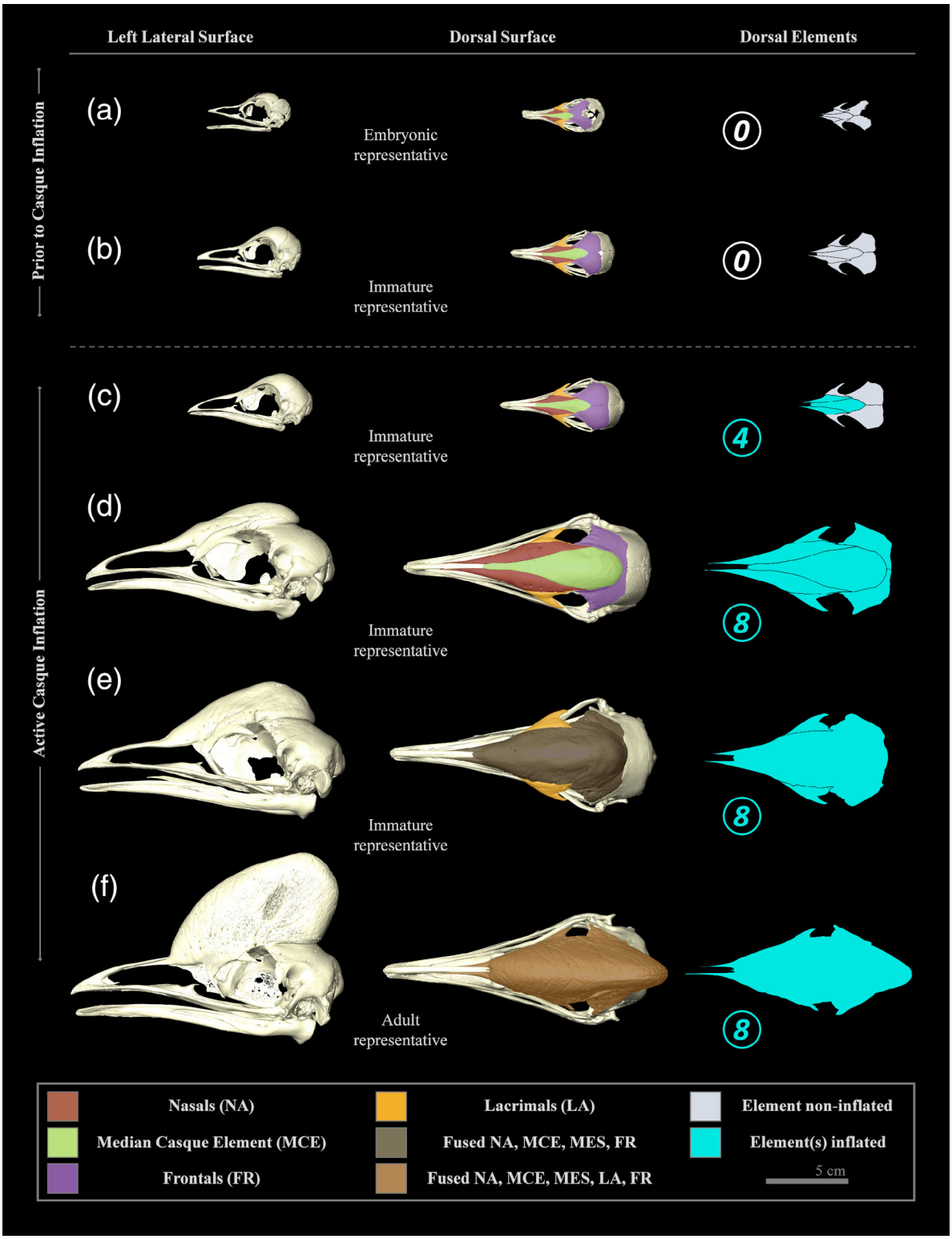

FIGURE 10 Sequence of casque development of *Casuarius casuarius* individuals from embryo to adult (a = embryo, ~HH40, TLG C032; b = immature, 1 day old, TLG C010; c = immature, 1.5 months old, TLG C037; d = immature, 14.0 months old, TLG C031; e = immature, ~24.0 months old, AMNH SKEL 963; f = adult, ~4.0–5.0 years, AMNH SKEL 962) in left lateral view (left column). Colors indicate casque bones and completed bony fusions (middle column), and pneumatic inflations (right column). (1) Casque bones: maroon = nasals, green = median casque element, orange = lacrimals, purple = frontals; (2) completed bony fusions: dark brown = NA (nasals) + MCE (median casque element) + MES (mesethmoid) + FR (frontals); light brown = NA + MCE + MES + FR + LA (lacrimals); and (3) pneumatic inflations: grey = non-inflated, light blue = inflated; circled. Encircled Arabic numbers indicate the number of inflated casque elements from 0 to 8 (this count includes the mesethmoid, which is not visible from the dorsal view). For additional specimen details, refer Data S1

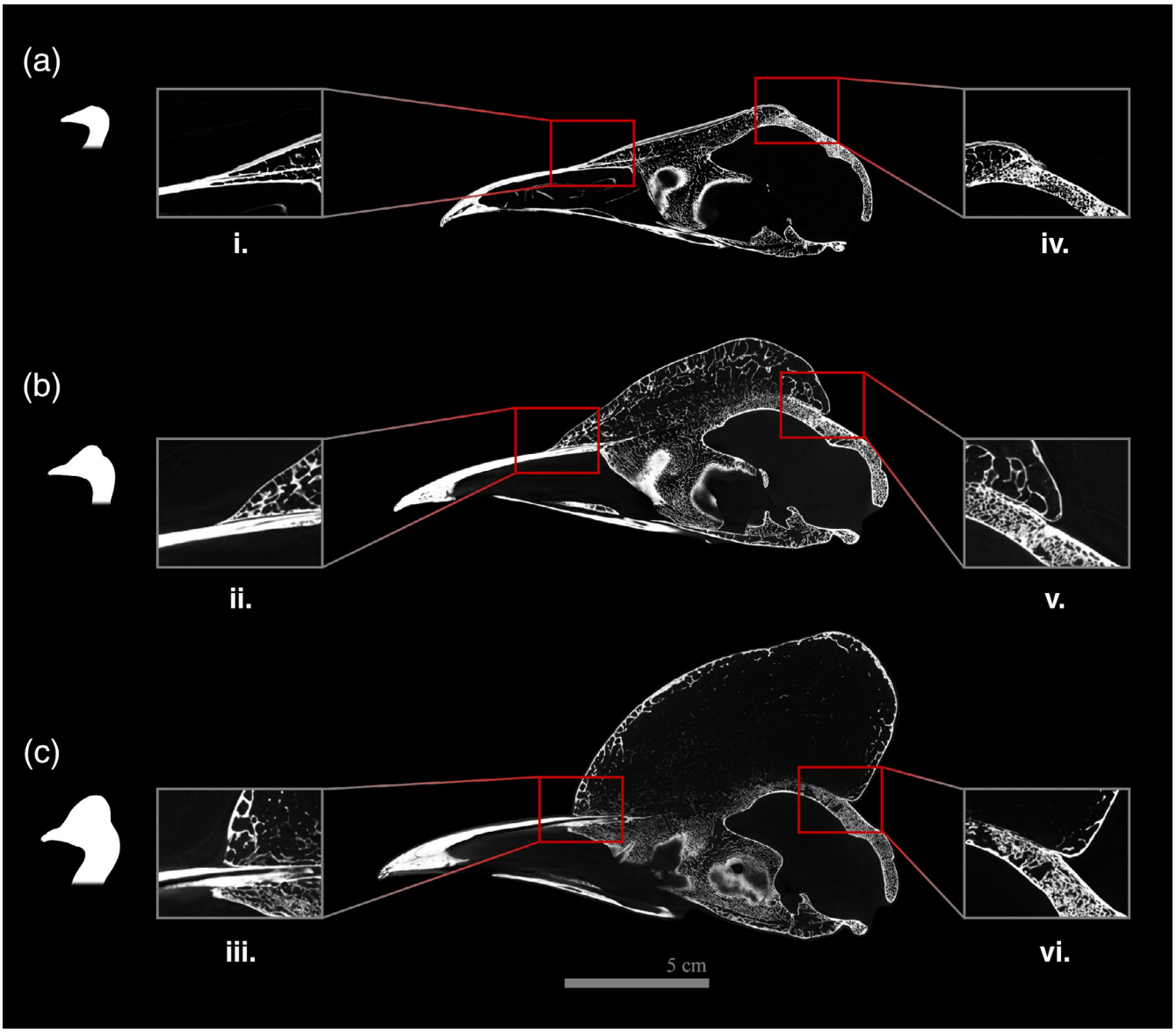

FIGURE 11 Osteological progression of *Casuarius casuarius* casques with parasagittal sections taken adjacent to the midline (a = immature, ~5.5 months, TLG C002; b = immature, ~24.0 months, AMNH SKEL 963; c = adult, ~4.0–5.0 years, AMNH SKEL 962). Smaller red rectangles contain areas of developmental casque folding, which are highlighted in larger grey rectangles for (i–iii) rostral folding over the caudodorsal process of the premaxilla and (iv–vi) caudal folding over the frontals. White silhouettes indicate progress in overall casque maturity for each individual; for additional specimen details, see Data S1

The individual at 14.0 months of age (Figures 4a and 9d–f; TLG C031; Data S1) clearly illustrates that each of the bony casque components is inflated (Figure 3). Notably, this is the latest stage in our sample at which sutures are fully to mostly patent between all casque cranial elements (Figures 3, 4a, 9d–f, and 10d). There is some internal remodeling that encompasses the median casque element with the mesethmoid, nasals, and frontals, respectively (Figure 4a). However, the surface furrows along sutures are deep (Figures 3 and 9d–f), and elements appear to be largely distinct in CT sections (Figure 4a). The nasals and median casque elements are more dorsally protrusive, and the median casque element has widened laterally (Figure 9) compared to the 10.4-month-old individual (TLG C004). The orbital processes of the lacrimals in this individual have expanded dorsally to further contribute to the overall casque inflation.

3.3.3 | Immature: Phase 3

Individuals in this phase have casque elements that are all inflated to some degree, and some elements are fused as indicated by obliterated sutures. By approximately

24.0 months of age (AMNH SKEL 963; Data S1) sutures between all bones contributing to the casque are largely obliterated (Figure 10e). The interior of the casque now appears as a single unit of well-pneumatized bone (Figure 11b) with thicker bony margins where suture contacts used to be. The last of the partially patent sutures include superficial aspects of the orbital processes of the lacrimals with the corresponding nasal and frontal as well as the superficial, rostralmost border between the median casque element and mesethmoid (Figure 10e). Simultaneously, the fused dorsal region (previously of nasals and mesethmoid origin), expands further dorsally, and the internal trabecular bone throughout all casque elements becomes more widely spaced (Figure 11b). It is also at approximately this point when the orbital processes of the lacrimals and the dorsalmost margins of the frontals have enlarged enough to play a more prominent role as the lateral base of the casque. Finally, the caudodorsal portion of the frontal has osteo-developmentally folded further caudally atop itself (Figures 10e and 11b, v).

3.4 | Bony cranial anatomy in adult specimens

The casques of mature individuals (>4.0 years of age) are the widest, extend furthest caudally atop the neurocranium, and are most dorsally protrusive. As observed in other studies (e.g., Flower, 1871; Mayr, 2018; Pycraft, 1900; Richardson, 1991), no patent sutures could be visualized on the external surfaces of the casque, nor could we detect internal sutures despite the use of μCT imaging (Figure 11c; AMNH SKEL 962; ∼4.0–5.0 years; also see Data S1). This is consistent with a high degree of bone remodeling that occurs during the fast period of casque inflation and expansion in the transitionary period between immaturity and maturity (Figure 10e,f). Within the internal trabeculae of the casque, there are thin, flattened sections of bone that differ from surrounding, sparse honeycombing, and these appear to be remnants of bone–bone interfaces at which internal sutures once occurred. As adults, the internal struts of trabecular bone become so widely spaced that in some areas largely air-filled voids are prominent. This is especially true in the central to caudal regions of the internal casque (Figure 11c, also see Naish & Perron, 2016). These observations contrast with the rostral region of the casque, which shows thicker cortices and larger struts of trabecular bone in adults. The casque is expanded further caudally via elongation of the nasals and median casque element (Figure 10f) along with osteo-developmentally folded frontals (Figure 11c, vi). Minor folding also occurs rostrally via inflation of the median casque element atop the caudodorsal process of the premaxilla (Figures 10f and 11a–c, i–iii). Note that the premaxilla is distinct from the casque as it is noninflated and does not fuse to any casque elements throughout ontogeny. As adults, casques may deviate from the midline, curving laterally to either the right or the left (Rothschild, 1900).

3.5 | Summary of inflations and fusions of the casque

It has been proposed that the developmental origin of casque pneumatization in *C. casuarius* is from the tympanic diverticula, through a series of tubes and compartments (Starck, 1995), rather than from the nasal sinuses. These passages appear to travel from the tympanic region through the quadrates, squamosals, and caudolateral bones of the cranium and into the frontal bones (Starck, 1995). Witmer (1990) mentions that a caudodorsal diverticulum of the antorbital sinus provides some pneumatization to the mesethmoid, frontals, or both in some birds. This is accompanied by additional pneumatization of the middle ear (Starck, 1995; Witmer, 1990). We do not observe obvious interactions of the antorbital sinus with the multi-element internal casque cavity (endocasque) in *C. casuarius*; however, a more detailed study of this potential mechanism should be completed with cassowaries to provide further clarity. Although the frontals are not the first elements to contribute to the inflation of the casque structure, they do appear to be the first to pneumatize. We hypothesize that pneumatization of the median casque element originates from partial caudal contact with the frontals. Additionally, the tympanic origin of these cranial pneumatic sinuses may supply the basiparasphenoid, passing along its parasphenoid rostrum and traversing dorsally to the inferior aspect of the mesethmoid (Witmer, 1990). Notably, our growth series indicates that the ventral portion of the interorbital septum of the mesethmoid does not contact the parasphenoid rostrum until *C. casuarius* have reached sub-adulthood (∼24.0 months of age; Figure 10e). Although the mesethmoid appears to begin pneumatization before this contact occurs, we cannot discount the contribution of the basiparasphenoid pneumaticity to subsequent mesethmoid inflation. Immature birds of ages 10.4 and 14.0 months (TLG C004 and TLG C031, respectively) in our study illustrate two small but characteristic dorsal swellings of the casque, which can be seen in lateral profile (Figure 9b,e). Although it is tempting to interpret this morphology as a result of two sources of pneumatization, it occurs prior to the contact between the parasphenoid rostrum and mesethmoid

(Figure 10e). Instead, we presume these surficial contours are from inflations of the nasals and median casque elements prior to their fusion. Once sutures between the nasals and the median casque element close (between 14.0 and 24.0 months of age), the casque morphology becomes more uniformly convex in appearance. After sutural fusion between all casque elements occurs beyond 24.0 months of age, dorsal expansion of the casque increases relatively rapidly (Figures 10e,f and 11b,c). Taken as a whole, we propose the sequence of incorporation of individual elements into the casque based on inflations and fusions is: (a) median casque element, (b) mesethmoid, (c) nasals, (d) frontals, and (e) lacrimals (Figure 10).

4 | DISCUSSION

4.1 | Gross morphology of the casque

Although several authors have described cassowary casques previously (Flower, 1871; Marshall, 1872; Mayr, 2018; Naish & Perron, 2016; Parker, 1866; Pycraft, 1900; Richardson, 1991; Table 1), a complete understanding of southern cassowary casque osteological composition has been elusive. Cranial μCT data comparing the largest growth series of *C. casuarius* to date ($n = 23$) allowed us to track bony elements and approximate the timing and sequence by which they are incorporated into the casque. We determined that the casques of cassowaries are composed of a greater variety of constituent parts than previously reported (Flower, 1871; Marshall, 1872; Mayr, 2018; Naish & Perron, 2016; Parker, 1866; Pycraft, 1900; Richardson, 1991). We find that the casque is composed of contributions of two midline and three paired bony elements: median casque element, mesethmoid, nasals, lacrimals, and frontals.

Additionally, we found that initiation of incipient casque growth occurs relatively early in development (i.e., by approximately 1.5 months of age; Figures 5a, iv and 8b). Dodson (1975) was the first study to analyze the cranial metrics of an ontogenetic series of cassowaries and provided support for the positive allometry of *Casuarius* casques after approximately 2 years of age. These data were used by Dodson (1975) to make comparisons of cranial ornament development between cassowaries and hadrosaur dinosaurs. Later, these data were further figured by Farke, Chok, Herrero, Scolieri, and Werning (2013) in a survey of ornamented archosaurs, showing that *Casuarius* ornaments are present during ontogeny by approximately 65–85% of adult body mass (i.e., roughly 2 years of age; Dodson, 1975). These studies provide a framework to compare the developmental timings of cranial ornaments across living and extinct taxa, and we believe our current study can contribute to this understanding by filling in the osteological timespan between neonate and subadult *C. casuarius* in which the dorsal expansion of the incipient casque appears and develops (Figures 5, 8, and 10).

4.2 | Reinterpretation of casque elements

No previous study has identified the same combination of bony elements within the cassowary casque as we have identified here (Flower, 1871; Mayr, 2018; Marshall, 1872; Naish & Perron, 2016; Parker, 1866; Pycraft, 1900; Richardson, 1991; Table 1). Notably, prior examinations of cassowary casques have relied extensively on visual inspection (Flower, 1871; Marshall, 1872; Mayr, 2018; Naish & Perron, 2016; Parker, 1866; Pycraft, 1900; Richardson, 1991), analyzed adult individuals only (Flower, 1871; Richardson, 1991), utilized solitary immature specimens for hallmark species descriptions (*C. bennetti*, Parker, 1866; *C. galetus* (= *C. casuarius*), Marshall, 1872; *C. unappendiculatus* and *C. sclaterii* (= *C. casuarius*), Pycraft, 1900), or sampled from unknown species/subspecies complexes (*C. casuarius* and *Casuarius* sp., Mayr, 2018). Having documented regional, multi-element fusion in the casque within our sample, we suspect that casque growth along with interspecific differences in casque shape (and potentially in configuration or sequence of inflation) may have historically obscured the southern cassowary pattern. These issues likely explain differences in the literature regarding casque composition over the last 150 years.

Regarding midline elements, multiple ossification centers of the mesethmoid (i.e., interorbital septum and lamina dorsalis) have been described previously for ratites (e.g., Maxwell, 2009). Our work identifies a similar ossification pattern in *C. casuarius* as has been described in *D. novaehollandiae* (Maxwell, 2009). Our data also illustrate that the mesethmoid is a contributor to casque formation (Figures 4 and 10), which was hypothesized in initial interpretations (Flower, 1871; Marshall, 1872; Parker, 1866; Pycraft, 1900) as well as more recent work (Mayr, 2018). We also find, however, that the identity of the dorsalmost structure of the casque is not the lamina dorsalis of the mesethmoid, but rather a separate element (Figures 3–5) identified herein as the median casque element (after Pycraft, 1900). The embryonic *C. casuarius* μCT data clearly show the gradual appearance of separate interorbital septum and lamina dorsalis ossification centers of the mesethmoid (Figure 5a, i–ii; TLG C032, ∼HH40; TLG C030, ∼HH41) from the more

dorsal element. Once visible, these centers fuse to one another over a relatively short period of embryogenesis: approximately 4 days (TLG C030, ~HH41 = two separate mesethmoid elements; TLG C005, ~HH43 = single fused mesethmoid; Data S1). As a result, the identities of these elements could be easily missed in post-hatching individuals. Our interpretation of the midline casque osteology is most consistent with Pycraft (1900), which includes the mesethmoid internally and the dorsalmost median casque element as an additional, midline contribution. This suggests that the median casque element may be neomorphic in cassowaries. Additional studies tracing the developmental and evolutionary origin of this bone may help elucidate the coincident appearance of the bone and the casque in exclusively cassowary lineages.

For bilateral casque elements, the lacrimal bones merit discussion. To the best of our knowledge, the lacrimals have only been recognized as potential elements of the casque by a single previous author (Flower, 1871), who described them from an adult specimen with casque sutures developmentally obliterated. We include the lacrimals as casque contributors based on μCT data, which illustrate that (a) the lacrimals contribute structurally to the lateral base of the casque in *C. casuarius* (Figures 3 and 10), and (b) the orbital processes of the lacrimals become inflated in concert with other casque contributors (Figure 4). Like the lacrimals, we also find the dorsalmost margins of the frontals contribute to the caudolateral regions of the casque base of southern cassowaries (Figures 3 and 10). Overall, the frontals provide an inferior platform for the caudalmost osteo-developmental folding that occurs (Figure 11a–c, iv–vi). The dorsalmost margins of the frontals first extend dorsally, and as other casque components expand caudodorsally, the frontals osteo-developmentally fold overtop themselves, even as caudal as the parietals, into adulthood (Figures 10 and 11c, vi). Some authors have not mentioned the frontals as casque-participating elements (Marshall, 1872; Mayr, 2018; Parker, 1866), which is understandable considering that the adult phenotype obliterates the boundaries between the frontals and adjacent bones. In addition, the bony growth of the folded frontals can appear externally as if it is a remnant suture between the casque and the braincase (Figure 2). Finally, previous studies have identified the nasals as elements largely contributing to the casque (Flower, 1871; Marshall, 1872; Mayr, 2018; Pycraft, 1900), which generally agrees with our findings for southern cassowaries. The premaxillary processes of the nasals are the only regions of these bones that do not become incorporated into the casque, instead of contributing to the dorsal border of the bony nasal aperture (Figures 3 and 10).

5 | CONCLUDING REMARKS

Cassowary casques are osteologically more complex than previously thought. Instead of one or three individual bones, the casque is composed of eight separate bony elements (Figure 3), including a possibly neomorphic median casque element. Moreover, this configuration appears to be unique among modern birds (see Maxwell, 2008, 2009; Mayr, 2018; Parker, 1866; Pycraft, 1900; Zusi, 1993). We recommend that future studies focus on other cassowary species to determine if the putative neomorphic midline casque element is present throughout the genus, as implied by Pycraft (1900). Notably, the taxonomy of *Casuarius* has been highly speculative, due in part to potential hybridization (e.g., through tribal trading and transport of birds to different ranges; see Perron, 2016). Clearly demonstrating that study specimens are of the same species, and not hybrids, will be critical for addressing potential differences in casque composition across *Casuarius*. We suspect this point will be particularly important not only for tracking homologous bones during embryogenesis and ontogeny in *C. unappendiculatus* and *C. bennetti*, but also for directly comparing cassowary species to other archosaurs. Finally, we anticipate that a newfound understanding of casque osteology will also aid future investigations into the potential biological role(s) of cassowary casques, specifically, as well as for better understanding the phenotypic complexities of osteological ornaments among tetrapods more generally (Bickel & Losos, 2002; Felice & Goswami, 2018; Jared et al., 2005; O'Brien et al., 2016).

ACKNOWLEDGMENTS

Funding for this study was provided by the National Science Foundation (1450850, 1457180, 1725925, and 1754659 to P. M. G.), OSU-CHS, Western Interior Paleontological Society (Karl Hirsh Memorial Grants), The Company of Biologists (and sponsoring journal, Experimental Biology, JEBTF1903122), and American Association of Anatomists (to T. L. G.). The authors thank AMNH (Bentley Bird, Paul Sweet, Thomas Trombone), CCP (R. Glenn Hood, Scott Snedeker), CG (Jay Young), DAER (Mark Corbridge, Tish Corbridge), DMNS (Garth Spellman, Jeff Stephenson, Andrew Doll), GPZ (Thomas DeMaar, Natalie Lindholm), HLB (Yulia Brockdorf, Rich McClure), KSM (Jeff Krehbiel), LNR (Stan Barenberg, Samantha Potts), MOO (Jay Villemarette, Michelle Hayer), MV (Ricky-Lee Erickson, Kylea Clarke), NHMUK (Hein Van Grouw, Mark Adams, Joanne Cooper, Judith White, Pete Key, Claire Walsh), OUVC (Larry Witmer), PBZ (Ashley Bowen, Kathy Wolyn, Katie Glatfelter), QM (Heather Janetzki, Kristen Spring, Alison Douglas), RCER (Linn Turner, Terry Turner), SCZ (Scott

Newland, Heather Arens, Phillip Horvey), SME (Joylene Reavis), VVE (Betty Lou Cauffman), and WEL (Steve Sarno, Adam Sarno) for access to and/or donation of specimens for this project. We appreciate assistance in specimen μCT imaging from AMNH (Morgan Hill, Andrew Smith), Dentsply (Steven Rigsby), MICRO (Manon Wilson), and OUμCT (Larry Witmer and Ryan Ridgely). The authors also thank CSU (Jeremy Delcambre, Robert Lee) and OSU-CHS for use of dissection and processing facilities. For helpful conversions regarding this study, we appreciate discussions with Haley O'Brien, Larry Witmer, Akinobu Watanabe, David Kay, Ryan Felice, Holly Ballard, Jennifer Volberding, Maria Bailey, Sue Ware, and Mark Norell. Additionally, we thank the American Emu Association for their contributions and support. We recognize the editorial team and anonymous reviewers for comments that improved this article.

AUTHOR CONTRIBUTIONS

Todd Green: Conceptualization; data curation; formal analysis; funding acquisition; investigation; methodology; resources; supervision; validation; visualization; writing-original draft; writing-review and editing. **Paul Gignac:** Conceptualization; data curation; formal analysis; funding acquisition; investigation; methodology; resources; supervision; validation; visualization; writing-original draft; writing-review and editing.

ORCID

Todd L. Green https://orcid.org/0000-0003-1407-6738
Paul M. Gignac https://orcid.org/0000-0001-9181-3258

REFERENCES

Baumel, J. J., & Witmer, L. M. (1993). Osteologia. In J. J. Baumel, A. S. King, J. E. Breazile, H. E. Evans, & J. C. vanden Berge (Eds.), *Handbook of avian anatomy: Nomina Anatomica Avium* (2nd ed., pp. 45–132). Cambridge: Nuttall Ornithological Club.

Bickel, R., & Losos, J. B. (2002). Patterns of morphological variation and correlates of habitat use in chameleons. *Biological Journal of the Linnean Society*, *76*(1), 91–103.

Bradford, M. G., & Westcott, D. A. (2010). Consequences of southern cassowary (*Casuarius casuarius*, L.) gut passage and deposition pattern on the germination of rainforest seeds. *Austral Ecology*, *35*(3), 325–333.

Bradford, M. G., & Westcott, D. A. (2011). Predation of cassowary dispersed seeds: Is the cassowary an effective disperser? *Integrative Zoology*, *6*(3), 168–177.

Brassey CA, O'Mahoney T. 2018. Pneumatisation and internal architecture of the Southern Cassowary *Casuarius casuarius* casque: A microCT study. Report from a BOU Funded Project. https://www.bou.org.uk/wp-content/uploads/2018/02/brassey.pdf

Crome, F. H. J., & Moore, L. A. (1988). The cassowary's casque. *EMU*, *88*(2), 123–124.

Dodson, P. (1975). Taxonomic implications of relative growth in lambeosaurine hadrosaurs. *Systematic Biology*, *24*(1), 37–54.

Eastick, D. L., Tattersall, G. J., Watson, S. J., Lesku, J. A., & Robert, K. A. (2019). Cassowary casques act as thermal windows. *Scientific Reports*, *9*(1), 1966.

Farke, A. A., Chok, D. J., Herrero, A., Scolieri, B., & Werning, S. (2013). Ontogeny in the tube crested dinosaur *Parasaurolophus* (Hadrosauridae) and heterochrony in hadrosaurids. *PeerJ*, *1*, e182.

Felice, R. N., & Goswami, A. (2018). Developmental origins of mosaic evolution in the avian cranium. *PNAS*, *115*(3), 555–560.

Flower, W. H. (1871). On the skeleton of the Australian cassowary (*Casuarius australis*). *Proceedings of the Zoological Society of London*, *3*, 32–35.

Hamburger, V., & Hamilton, H. L. (1951). A series of normal stages in the development of the chick embryo. *Journal of Morphology*, *88*(1), 49–92.

Heather, B., & Robertson, A. (1997). *The field guide to the birds of New Zealand*. Oxford: Oxford University Press. ISBN-10: 0198501463; ISBN-13: 978-0198501466.

Jared, C., Antoniazzi, M. M., Navas, C. A., Katchburian, E., Freymüller, E., Tambourgi, D. V., & Rodrigues, M. T. (2005). Head co-ossification, phragmosis and defence in the casque-headed tree frog *Corythomantis greeningi*. *Journal of Zoology*, *265*(1), 1–8.

Kesteven, H. L. (1942). The ossification of the avian chondrocranium, with special reference to that of the emu. *Proceedings of the Linnean Society of NSW*, *67*, 213–237.

Kofron, C. P. (1999). Attacks to humans and domestic animals by the southern cassowary (*Casuarius casuarius johnsonii*) in Queensland, Australia. *Journal of Zoology*, *249*(4), 375–381.

Mack, A. L. (1995). Distance and non-randomness of seed dispersal by the dwarf cassowary *Casuarius bennetti*. *Ecography*, *18*(3), 286–295.

Mack, A. L., & Jones, J. (2003). Low-frequency vocalizations by cassowaries (*Casuarius* spp.). *The Auk*, *120*(4), 1062–1068.

Marchant, S., & Higgins, P. J. (1990). *Handbook of Australian, New Zealand and Antarctic birds. Vol. 1 Ratites to Ducks*. Melbourne: Oxford University Press. ISBN-10: 0195530683; ISBN-13: 978-0195530681.

Marshall, W. (1872). Über die knöchernen Schädelhöcker der Vögel. *Neiderländischens Archiv fiir Zoologie*, *1*, 133–179.

Maxwell, E. E. (2008). Ossification sequence of the avian order Anseriformes, with comparison to other precocial birds. *Journal of Morphology*, *269*(9), 1095–1113.

Maxwell, E. E. (2009). Comparative ossification and development of the skull in palaeognathous birds (Aves: Palaeognathae). *Zoological Journal of the Linnean Society*, *156*(1), 184–200.

Mayr, G. (2018). A survey of casques, frontal humps, and other extravagant bony cranial protuberances in birds. *Zoomorphology*, *137*, 457–472.

Minnaar, P., & Minnaar, M. (1992). *The emu farmer's handbook* (Vol. 1). Groveton, TX: Induna Publishing Co. ISBN-10: 0964374110; ISBN-13: 9780964374119.

Minnaar, P., & Minnaar, M. (1998). *The emu farmer's handbook* (Vol. 2). Groveton, TX: Nyoni Publishing Co. ISBN-10: 0964374145; ISBN-13: 9780964374140.

Nagai, H., Mak, S. S., Weng, W., Nakaya, Y., Ladher, R., & Sheng, G. (2011). Embryonic development of the emu,

Dromaius novaehollandiae. *Developmental Dynamics*, *240*(1), 162–175.

Naish, D., & Perron, R. (2016). Structure and function of the cassowary's casque and its implications for cassowary history, biology and evolution. *Historical Biology*, *28*(4), 507–518.

O'Brien, H. D., Faith, J. T., Jenkins, K. E., Peppe, D. J., Plummer, T. W., Jacobs, Z. L., ... Tryon, C. A. (2016). Unexpected convergent evolution of nasal domes between Pleistocene bovids and cretaceous hadrosaur dinosaurs. *Current Biology*, *26*(4), 503–508.

Olson, V. A., & Turvey, S. T. (2013). The evolution of sexual dimorphism in New Zealand giant moa (*Dinornis*) and other ratites. *Proceedings of the Royal Society B*, *280*(1760), 20130401.

Parker, W. K. (1866). VIII. On the structure and development of the skull of the ostrich tribe. *Proceedings of the Zoological Society of London*, *14*, 112–114.

Perron, R. M. (2016). *Taxonomy of the genus Casuarius: The defined and known living cassowary species and subspecies*. Berkshire, UK: Quantum Conservation. ISBN-10: 3865232728; ISBN-13: 978-3865232724.

Phillips, P. K., & Sanborn, A. F. (1994). An infrared, thermographic study of surface temperature in three ratites: Ostrich, emu and double-wattled cassowary. *Journal of Thermal Biology*, *19*(6), 423–430.

Pycraft, W. P. (1900). On the morphology and phylogeny of the palæognathæ (ratitæ and crypturi) and neognathæ (carinatæ). *Transactions of the Zoological Society of London*, *15*(5), 149–290.

Richardson, K. C. (1991). The bony casque of the Southern Cassowary *Casuarius*. *EMU*, *91*, 56–51, 58.

Romagnano, A., Hood, R. G., Snedeker, S., & Martin, S. G. (2012). Cassowary pediatrics. *Veterinary Clinics: Exotic Animal Practice*, *15*(2), 215–231.

Rothschild, W. (1900). A monograph of the genus *Casuarius*. *Transactions of the Zoological Society of London*, *15*(5), 109–148.

Starck, J. M. (1995). Comparative anatomy of the external and middle ear of Palaeognathous birds. *Advances in Anatomy, Embryology, and Cell Biology*, *131*, 1–137.

Stocker, G. C., & Irvine, A. K. (1983). Seed dispersal by cassowaries (*Casuarius casuarius*) in North Queensland's rainforests. *Biotropica*, *15*, 170–176.

Webber, B. L., & Woodrow, I. E. (2004). Cassowary frugivory, seed defleshing and fruit fly infestation influence the transition from seed to seedling in the rare Australian rainforest tree, *Ryparosa* sp. nov. 1 (Achariaceae). *Functional Plant Biology*, *31*(5), 505–516.

Witmer, L. M. (1990). The craniofacial air sac system of Mesozoic birds (Aves). *Zoological Journal of the Linnean Society*, *100*(4), 327–378.

Zusi, R. L. (1993). Patterns of diversity in the avian skull. In J. Hanken & B. K. Hall (Eds.), The Skull *Patterns of structural and systematic diversity* (Vol. 2, pp. 391–437). Chicago, IL: University of Chicago Press.

SUPPORTING INFORMATION

Additional supporting information may be found online in the Supporting Information section at the end of this article.

How to cite this article: Green TL, Gignac PM. Osteological description of casque ontogeny in the southern cassowary (*Casuarius casuarius*) using micro-CT imaging. *Anat Rec*. 2020;1–19. https://doi.org/10.1002/ar.24477